scientific reports

Check for updates

OPEN

Ssc-miR-101-3p inhibits hypoxia-induced apoptosis and inflammatory response in alveolar type-II epithelial cells of Tibetan pigs via targeting *FOXO3*

Haonan Yuan[1], Xuanbo Liu[1], Binpeng Xi[1], Caixia Gao[2], Jinqiang Quan[1], Shengguo Zhao[1] & Yangnan Yang[1]✉

Tibetan pigs are a unique swine strain adapted to the hypoxic environment of the plateau regions in China. The unique mechanisms underlying the adaption by Tibetan pigs, however, are still elusive. Only few studies have investigated hypoxia-associated molecular regulation in the lung tissues of animals living in the plateau region of China. Our previous study reported that ssc-miR-101-3p expression significantly differed in the lung tissues of Tibetan pigs at different altitudes, suggesting that ssc-miR-101-3p plays an important role in the adaptation of Tibetan pigs to high altitude. To understand the underlying molecular mechanism, in this study, the target genes of ssc-miR-101-3p and their functions were analyzed via various methods including qRT-PCR and GO and KEGG pathway enrichment analyses. The action of ssc-miR-101-3p was investigated by culturing alveolar type-II epithelial cells (ATII) of Tibetan pigs under hypoxic conditions and transfecting ATII cells with vectors overexpressing or inhibiting ssc-miR-101-3p. Overexpression of ssc-miR-101-3p significantly increased the proliferation of ATII cells and decreased the expression of inflammatory and apoptotic factors. The target genes of ssc-miR-101-3p were significantly enriched in FOXO and PI3K-AKT signaling pathways required to mitigate lung injury. Further, *FOXO3* was identified as a direct target of ssc-miR-101-3p. Interestingly, ssc-miR-101-3p overexpression reversed the damaging effect of *FOXO3* in the ATII cells. In conclusion, ssc-miR-101-3p targeting *FOXO3* could inhibit hypoxia-induced apoptosis and inflammatory response in ATII cells of Tibetan pigs. These results provided new insights into the molecular mechanisms elucidating the response of lung tissues of Tibetan pigs to hypoxic stress.

Keywords Tibetan pigs, Hypoxia, Ssc-miR-101-3p, Alveolar type-II epithelial cells, *FOXO3*

The Qinghai-Tibet Plateau is known as the "roof of the world" and "water tower of Asia." It is the highest plateau in the world[1,2]. It has a unique environment with low temperature, low oxygen, low pressure, and strong ultraviolet radiation. When people living at low altitude enter the plateau, some may develop a series of nonspecific symptoms and syndromes including headache, fatigue, vomiting, chest tightness, and nausea due to poor acclimatization, which is called acute altitude sickness[3]. Altitude sickness is the most obvious initial symptom of change in lung function. Alveolar hypoxia is the most significant feature of high-altitude environment[4]. Long-term exposure to high altitude and low-oxygen environment affects the cardiopulmonary system, which can eventually lead to pulmonary hypertension and pulmonary edema[5]. Tibetan pig is a unique local pig breed in the plateau areas of China. Tibetan pigs live in high-altitude areas with low temperature and low oxygen for a long time, and they have developed a unique mechanism to adapt to the extreme environment of the plateau[6,7]. Under hypoxia, investigation of the molecular mechanisms in the lungs of these pigs, as a representative model animal in high-altitude areas, can help in developing strategies for humans or other animals to adapt to hypoxic environment at high altitudes.

[1]College of Animal Science and Technology, Gansu Agricultural University, Lanzhou, China. [2]State Key Laboratory of Veterinary Biotechnology, Harbin Veterinary Research Institute, Chinese Academy of Agricultural Sciences, Harbin, China. ✉email: yangyn@gsau.edu.cn

MicroRNAs (miRNAs), approximately 22 nucleotides in length, are non-coding RNAs that predominantly function through the pairing of their seed region—typically comprising the 2nd to the 7-8th nucleotides—with complementary sequences in the 3' untranslated regions (3'UTRs) of target mRNAs. This interaction leads to the formation of the RNA-induced silencing complex (RISC), resulting in gene expression suppression[8,9]. Studies demonstrate that miRNAs are indispensable components of various physiological processes, encompassing cell proliferation[10], oxidative stress, and apoptosis[11]. They further engage in complex regulatory mechanisms, notably by hindering translation initiation through competition with cap-binding proteins via miRNA-loaded Ago proteins, influencing mRNA circularization[12]. Our investigation delves deeply into the role of miRNAs in lung injury precipitated by hypoxia, resonating with insights into the protective effect of the miR-144/GSK3β axis[13], the modulation of HIF2α by miR-223[14], and the exacerbation of lung damage by miR-145[15]. Preliminary miRNA sequencing in Tibetan pig lungs reveals a striking variation in ssc-miR-101-3p expression correlated with altitude, suggesting its engagement in the adaptation to high-altitude environments[16] (Fig. 1G, Supplementary Table S1).

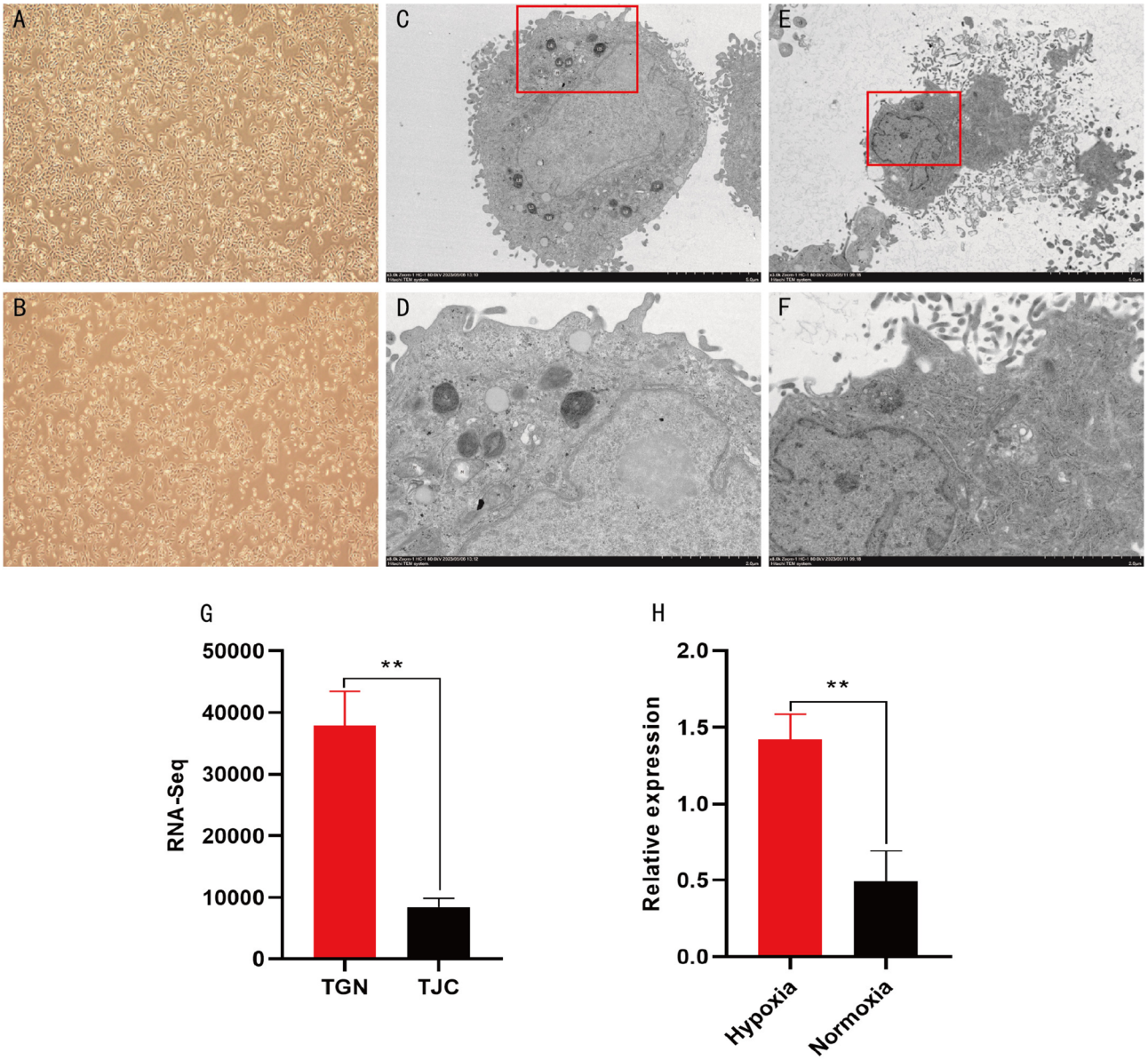

Fig. 1. Morphological observation of ATII cells. (**A**) ATII cell morphology after 48 h treatment in the normal oxygen group (10×). (**B**) ATII cell morphology after 48 h treatment in the hypoxia group (10×). (**C**) The internal structure of ATII cells in the normoxic group 48 h after the treatment (5 μm). (**D**) Enlarged structure of ATII cells at specific locations in the normoxic group 48 h after the treatment (2 μm). (**E**) The internal structure of ATII cells in the hypoxic group 48 h after the treatment (5 μm). (**F**) Enlarged structure of ATII cells at specific locations in the hypoxic group 48 h after the treatment (2 μm). (**G**) The expression of ssc-miR-101-3p in the lungs of TGN and TJC as evaluated by RNA-seq. (**H**) qRT-PCR was used to evaluate the expression of ssc-miR-101-3p in the ATII cells in the normoxic and hypoxic groups. microvilli (Mv), nucleus (N), mitochondria (M), and lamellar bodies (LB) are indicated. $^{*}P<0.05$, $^{**}P<0.01$ (the same below).

FOXO3 is a member of the Forkhead box O (FOXO) family of transcription factors. It regulates multiple biological processes including oxidative stress response, apoptosis, autophagy, proliferation, and immunity, thus playing an important role in cell fate determination[17–19]. In recent years, several studies have focused on the regulation of *FOXO3* by miRNAs. Yin et al. reported that miRNA-96-5p may play a tumor-promoting role by negatively regulating *FOXO3* to promote cell proliferation[20]. Cao et al. reported that miR-182-5p activates the Wnt signaling pathway by inhibiting the degradation of β-catenin and enhancing the interaction between β-catenin and *TCF4*; this is mediated by repressed *FOXO3a* so that miR-182-5p promotes the proliferation of hepatocellular carcinoma (HCC)[21]. Meng et al. reported that hypoxia can promote the upregulation of miR-155 in extracellular vesicles (EVs) inhibit the expression of *FOXO3*, and promote the proliferation of RCC cells, thereby promoting the progression of cell tumors[22].

Alveolar type-II epithelial cells (ATII) are one of the important cells constituting the alveolar epithelium, and they play an important role in maintaining the structure and function of the alveoli[23,24]. However, although *FOXO3* plays an important regulatory role in various types of apoptosis, its mechanism of action in ATII cells in Tibetan pigs under hypoxic conditions remains unclear. Therefore, in this study, we aimed to assess the effect of the miR-101/FOXO3 regulatory axis on the ATII cells in Tibetan pigs during hypoxic conditions. In addition, the target genes of ssc-miR-101-3p and their functions were predicted using three bioinformatic software to analyze the molecular mechanism of hypoxia-induced lung injury. This study would enhance the understanding of the regulation of miRNAs in lung injury under hypoxia.

Materials and methods

Ethics approval

The present study and all experimental techniques, including animal experiments, were approved by the Animal Ethics Committee of Gansu Agricultural University (GSAU-ETH-AST-2021-023), and comply with the relevant guidelines and regulations of ARRIVE.

Animal sample collection

Initially, 20 unrelated depopulated 6-month-old Tibetan pigs of similar weight were selected from Gannan Tibetan Autonomous Prefecture (Gannan, China). Among them, 10 Tibetan pigs were randomly selected for rearing in Gannan Tibetan Autonomous Prefecture. They were labeled as TGN, representing an altitude of 3000 m. The remaining 10 Tibetan pigs were moved from their native place in Gannan to Jingchuan County. They were labeled as TJC, representing an altitude of 1000 m, and reared under the same conditions as those for TGN for 6 months. Then, three pigs in each group were randomly selected for euthanasia by intramuscular injection of ketamine, and the left lower lung lobe was collected and rapidly frozen in liquid nitrogen for later RNA extraction and miRNA-seq[16,25].

Cell culture

One newborn (7-day-old) Tibetan pig was selected, anesthetized, and aseptically sacrificed. The lung tissue was collected. Primary ATII cells were isolated from the lungs according to the method described by Yang et al[16]. The isolated ATII cells were randomly divided into two groups: the control group (21% O_2, normoxia) and the experimental group (2% O_2, hypoxia). ATII cells were cultured under normoxic (74% N_2, 5% CO_2, and 21% O_2) or hypoxic (93% N_2, 5% CO_2, and 2% O_2) conditions using a mixed three-gas incubator(ESCO, Singapore). For dual-luciferase reporter assay, HEK-293T cells were purchased from the cell bank of the Chinese Academy of Sciences. These cells were cultured in Dulbecco's Modified Eagle Medium (DMEM, high glucose, HyClone, USA), supplemented with 12% (v/v) heat-inactivated GIBCO Fetal Bovine Serum (FBS, Thermo Fisher Scientific, USA), and 1% Penicillin–Streptomycin solution (Solarbio, Beijing).

Cell transfection

MiR-101 mimic (100 nM), mock negative control (NC; 100 nM), miR-101 inhibitor (50 nM), inhibitor NC (50 nM), small interfering RNA targeting *FOXO3* (si-FOXO3), and control siRNA (150 nM) were synthesized by GEMA Pharmaceutical Technology (Shanghai, China). *FOXO3* overexpression vector (pc-FOXO3; 1 μg) and pcDNA3.1 vector were purchased from GENEWIZ (Suzhou, China). When the ATII cells attained 80% confluency, they were transfected with miR-101-3p mimics, inhibitors, or their respective NCs using INVI DNA RNA Transfection Reagent™ (Invigentech, CA, USA) for 48 h. The details of miR-101 mimics, inhibitors, and si-FOXO3 with their respective NC sequences are given in Supplementary Table S2.

Cell proliferation assay

First, the cell viability was determined as follows. The transfected ATII cells were seeded in a 96-well plate at a density of 3×10^3 cells in 100 μL/well and incubated for 48 h. Further, 10 μL CCK-8 reagent (Solarbio, Beijing, China) was added to each well, and the plate was incubated at 37 °C for 2 h. The optical density (OD) was measured at 450 nm with an enzyme marker.

Cell proliferation was assessed using the BeyoClick EdU Cell Proliferation Kit (EdU, Beyotime, Shanghai, China) with Alexa Fluor 555. The transfected ATII cells were incubated with 10 μM EdU solution in growth medium for 3 h. The cells were stained with Hoechst 33,342 solution (blue) and observed under a fluorescent microscope (Olympus IX71, Tokyo, Japan) at 200 × magnification. EdU-positive cells were analyzed using ImageJ 1.6 software (National Institute of Health, USA).

Determination of cell cycle phase

The transfected ATII cells were seeded in six-well plates at the appropriate density for 48 h. The supernatant was discarded, and the cells were washed twice with PBS. Pre-chilled 70% alcohol was added to the cell suspension and incubated overnight at 4 °C. The cell cycle phase was determined as described previously[26]. The cell samples were centrifuged, and ethanol was removed. The cells were washed once with PBS, and 500 µL PBS was added to the cells. Further, the cells were resuspended in PBS and sent to Sevier Biotechnology Co., LTD (Wuhan, China) for apoptosis assay.

Cytotoxicity assay

The extent of cell damage was assessed by detecting the release of lactate dehydrogenase (LDH). ATII cells were inoculated in 24-well plates at a density of 1×10^5 cells/well and incubated for 24 h. When the cells attained approximately 70% confluency, miR-101 mimics, mimic NC, and miR-101 inhibitor or inhibitor NC were used to transfect the cells. The cells were incubated for 48 h, after which the medium was collected. The LDH activity in the supernatant was analyzed using LDH assay kit according to the manufacturer's instructions (Nanjing Jincheng Institute of Biological Engineering, Nanjing, China). The absorbance was measured at 450 nm with an enzyme marker (Thermo Fisher Scientific).

To determine the levels of reactive oxygen species (ROS), the cells were washed with PBS. DCFH-DA probe diluted in 10 µmol/L serum-free cell culture medium (Gibco, USA) was added to each well and incubated for 20 min at 37 °C. The cells were washed three times with serum-free cell culture medium to fully remove the DCFH-DA that did not enter the cells. Further, the fluorescence was observed under a fluorescence microscope.

Quantitative real-time PCR (*qRT-PCR*)

Total RNA was extracted from ATII cells using AG RNAex Pro RNA Extraction Reagent (AG, Hunan, China) according to the manufacturer's instructions. Mir-X miRNA First Strand Synthesis Kit and Evo M-MLV RT Kit and gDNA clean cDNA (AG, Hunan, China) were used to reverse transcribe the isolated RNA into complementary DNA (cDNA) for miRNA and mRNA expression analysis. The cDNA was stored at − 20 °C. qRT-PCR was performed using 2 × RealStar Fast SYBR qPCR Mix (GeneStar, Beijing, China) and LightCycler 480 II instrument (Roche, Basel, Switzerland). *β-actin* and U6 were used as internal mRNA and miRNA references, respectively. Data were obtained from three independent experiments. Relative expression levels were determined using the $2^{-\Delta\Delta Ct}$ method[27]. All primers were synthesized by Shanghai Prime Tech Biotechnology Co., Ltd (Shanghai, China), and the sequences are given in Table 1.

Western blot analysis

ATII cells were seeded in 6-well plates and transfected for 48 h using RIPA buffer and protease inhibitor mixture (Beyotime, Shanghai, China). All procedures were performed according to the kit instructions. Protein concentrations were determined using the BCA protein concentration assay kit (Servicebio, Wuhan, China). For each sample, equal concentration of protein was denatured using 4 × SDS-PAGE loading buffer. The denatured protein samples were separated by 10% SDS-PAGE and transferred to PVDF membranes. After blocking the PVDF membranes with 5% skim milk for 2 h at room temperature, the membranes were incubated with anti-FOXO3 (1:1000; GB11092-1, Servicebio, Wuhan, China) and anti-GAPDH (1:2000; GB15002, Servicebio) antibodies overnight at 4 °C. The next day, the PVDF membranes were washed 5 times with TBST and incubated with goat anti-rabbit horseradish peroxidase (HRP) IgG antibody (Servicebio) at room temperature for 1 h. After 3

Gene	Primer sequence(5`-3`)	Accession no.	Species
miR-101-3p	Forward:TCGCGTACAGTACTGTGATAACTGACT Reverse: mR Q 3'Primer(Universal downstream primers)	AJ459730	*Sus scrofa*
FOXO3	Forward:ACAAACGGCTCACTCTGTCCCA Reverse: GAACTGTTGCTGTCGCCCTTATC	XM_021084231.1	*Sus scrofa*
Bax	Forward: GCTGACGGCAACTTCAACTG Reverse: GCGTCCCAAAGTAGGAGAGG	XM_013998624.2	*Sus scrofa*
Bcl-2	Forward: GGTGAACTGGGGGAGGATTG Reverse: GTGCCGGTTCAGGTACTCAG	XM_021099593.1	*Sus scrofa*
IL-1β	Forward: TGATGCCAACGTGCAGTCTA Reverse: GGAGAGCCTTCAGCATGTGT	NM_001302388.2	*Sus scrofa*
IL-6	Forward: AACCTGAACCTTCCAAAAATGG Reverse: ACCGGTGGTGATTCTCATCA	NM_214399.1	*Sus scrofa*
IL-8	Forward: CTGCAGCTCTCTGTGAGGCTGC Reverse: TCCTTGGGGTCCAGGCAGACC	NM_213867.1	*Sus scrofa*
TNF-α	Forward: GCACTGAGAGCATGATCCG Reverse: AACCTCGAAGTGCAGTAGG	NM_214022.1	*Sus scrofa*
β-actin	Forward: ATATTGCTGCGCTCGTGGT Reverse: TAGGAGTCCTTCTGGCCCAT	AJ312193.1	*Sus scrofa*
U6	Forward: GGAACGATACAGAGAAGATTAGC Reverse: TGGAACGCTTCACGAATTTGCG	NC_000015	*Sus scrofa*

Table 1. Primers for qRT-PCR.

washes with TBST for 5 min each, the protein bands on the PVDF membranes were visualized using enhanced chemiluminescence (ECL) and a gel imaging system (Bio-Rad, Foster City, CA, USA). The grayscale values were analyzed using Image J software (http://imagej.nih.gov/ij/).

Bioinformatic analysis

To predict the targets of ssc-miR-101-3p in Sus scrofa, we leveraged an integrated suite of online tools including RNAhybrid (v2.1.2) alongside svm_light (v6.01), TargetScan (v7.0), and Miranda (v3.3a). With a dedicated focus on the 3'-UTR regions to circumvent potential false positives arising from non-specific mRNA binding sites, we prioritized 8mer and 7mer-m8 targets—deemed by TargetScan as high-confidence candidates. Applying stringent criteria of low binding energy and superior sequence complementarity, we refined our predictions. Post-prediction, we characterized the biological functions of these targets through meticulous Gene Ontology (GO) analysis and insightful scatter plot visualizations from the Kyoto Encyclopedia of Genes and Genomes (KEGG) pathways[28,29]. Employing a one-tailed hypergeometric test, we precisely pinpointed significantly enriched terms among the ssc-miR-101-3p target genes. To ensure robust q-values, we subjected the initial p-values to a stringent Bonferroni correction, mitigating the risk of false positives stemming from multiple comparisons. We emphasized terms that maintained significance post-correction ($P < 0.05$), utilizing a background gene set specific to the cell lines under investigation to maintain relevance and specificity. Consequently, *FOXO3* emerged as a preeminent candidate target gene of ssc-miR-101-3p, deserving of further in-depth inquiry.

Dual-luciferase reporter assay

HEK-293 T cells were inoculated in 24-well plates, and miR-101-3p or mock NC and FOXO3-WT or FOXO3-MUT were used to co-transfect the cells with confluency of 70%–80%. Luciferase activity was analyzed 48 h after transfection using a dual luciferase reporter kit (Promega, Madison, WI, USA) and normalized to Renilla luciferase activity values. Data were obtained from three independent experiments.

Statistical analysis

Graphs were plotted using GraphPad Prism 8.0 (GraphPad Software, San Diego, CA), and all data were presented as mean ± SEM. Differences between groups were analyzed using two-tailed student's t-test and one-way analysis of variance (ANOVA). $^{*}P < 0.05$ and $^{**}P < 0.01$ were considered significant and highly significant, respectively.

Ethics statement

The study and all experimental techniques were approved by the Ethics Committee for the Care and use of Laboratory Animals of Gansu Agricultural University (GSAU-ETH-AST-005). The experiments were performed in accordance with the relevant guidelines and regulations implemented by the Administration of Laboratory Animal Affairs approved by the National Science and Technology Commission on October 31, 1988.

Results

Morphological changes in the ATII cells under hypoxia

First, observe the morphological changes in ATII cells following hypoxia treatment. Compared to the normoxia group (Fig. 1A), the intercellular gaps in the hypoxia group widened, and more floating cells and cell debris were observed in the culture medium (Fig. 1B). Additionally, the ultrastructure of ATII cells was examined using transmission electron microscopy. After 48 h under normoxia, the intracellular and mitochondrial membranes in ATII cells were intact, and some concentric lamellar vesicles were visible (Fig. 1C, D). However, in the hypoxia group, the nuclei were irregular in shape. Most mitochondria were swollen; cristae were disrupted; lamellar vesicles were absent; autophagic vesicles formed, and signs of apoptosis were more pronounced (Fig. 1E, F).

Expression analysis of ssc-miR-101-3p

Ssc-miR-101-3p expression was determined in the lung tissue of Tibetan pigs at different altitudes. Pre-sequencing results of indicated that ssc-miR-101-3p expression was significantly higher in TGN than in TJC ($P < 0.01$; Fig. 1G; Supplementary Table S11). The results of qRT-PCR showed that in the hypoxia group, ssc-miR-101-3p expression was significantly elevated in ATII cells compared with the normoxia group ($P < 0.05$; Fig. 1H), which was consistent with the sequencing results. Therefore, ssc-miR-101-3p may play an important regulatory role in the lung tissue of Tibetan pigs under hypoxia.

Overexpression of ssc-miR-101-3p inhibits hypoxia-induced apoptosis of ATII cells in Tibetan pigs

Proliferation of ATII cells is crucial for the pulmonary adaptation to hypoxic environments[30]. To assess the regulatory role of ssc-miR-101-3p in the proliferation of ATII cells, methods such as CCK-8 assay, EdU staining, flow cytometry, and qPCR were employed. Following transfection with ssc-miR-101-3p mimics, inhibitors, and their respective NCs, there was a significant increase or decrease in the expression levels of ssc-miR-101-3p in ATII cells (Fig. 2A). Results from CCK-8 and EdU staining indicated that overexpression of ssc-miR-101-3p significantly enhanced cellular viability and proliferation of ATII cells, whereas knockdown of ssc-miR-101-3p exhibited the opposite effects (Fig. 2B,E,F). Flow cytometry results demonstrated that overexpression of ssc-miR-101-3p significantly increased the proportion of ATII cells in the G2 phase and decreased the proportion in the G1 phase (Fig. 2C,D). However, inhibition of ssc-miR-101-3p significantly reduced the proportion of cells in the S phase (Fig. 2C,D). Additionally, qRT-PCR analysis was used to examine the effects of ssc-miR-101-3p

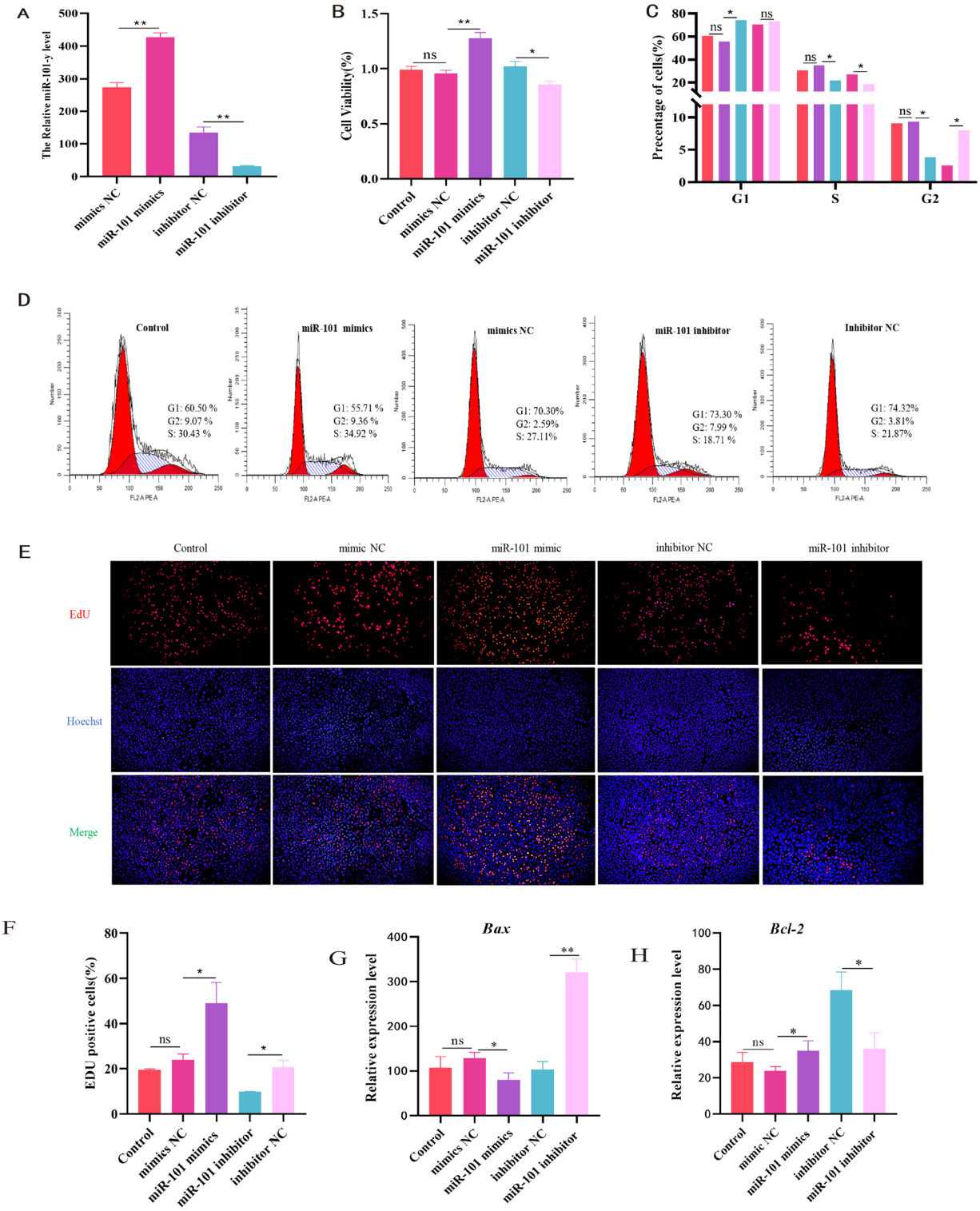

Fig. 2. Ssc-miR-101-3p overexpression promoted the proliferation of ATII cells. (**A**–**H**) ATII cells were transfected with simulated NC (100 nM), miR-101 mimics (100 nM), inhibitor NC, and miR-101 inhibitor (50 nM) and incubated for 48 h. (**A**) Transfection efficiency of miR-101 compared with control group. (**B**) CCK-8 assay was performed to analyze cell viability. The absorbance was measured at 450 nm. (**C**) Analysis of cell cycle phases. (**D**) Flow cytometric analysis of cell cycle. **(E)** Number of cells testing positive for EdU, DNA-replicating cells stained with EdU (red), and nuclei stained with Hoechst (blue). (**F**) Proportion of EdU-positive cells. (**G**–**H**) qRT-PCR was used to detect the mRNA levels of apoptosis-related genes *Bax* and *Bcl-2* after miR-101-3p transfection.

on the expression of apoptotic factors *Bax* and *Bcl-2*. After transfection with ssc-miR-101-3p mimics, *Bcl-2* was upregulated and Bax was downregulated, with trends reversing following ssc-miR-101-3p silencing (Fig. 2G,H).

Ssc-miR-101-3p attenuates hypoxia-induced inflammatory damage in the ATII cells

Living at high altitudes can lead to respiratory difficulty and pulmonary tissue infections in animals, primarily due to inflammatory damage in ATII cells. To explore the impact of ssc-miR-101-3p on the inflammatory processes in ATII cells, these cells were transfected with ssc-miR-101-3p mimics, inhibitors, or their respective NCs. Overexpression of ssc-miR-101-3p significantly inhibited LDH activity and reduced levels of ROS, while inhibition of ssc-miR-101-3p increased LDH activity and ROS levels (Fig. 3A,B). Furthermore, overexpression of ssc-miR-101-3p significantly lowered the transcription levels of inflammatory factors (*TNF-α*, *IL-1β*, *IL-6*, and *IL-8*); conversely, inhibition of ssc-miR-101-3p significantly increased the expression levels of these inflammatory factors. ssc-miR-101-3p may regulate the expression of inflammation-related genes and mitigate inflammatory damage in ATII cells.

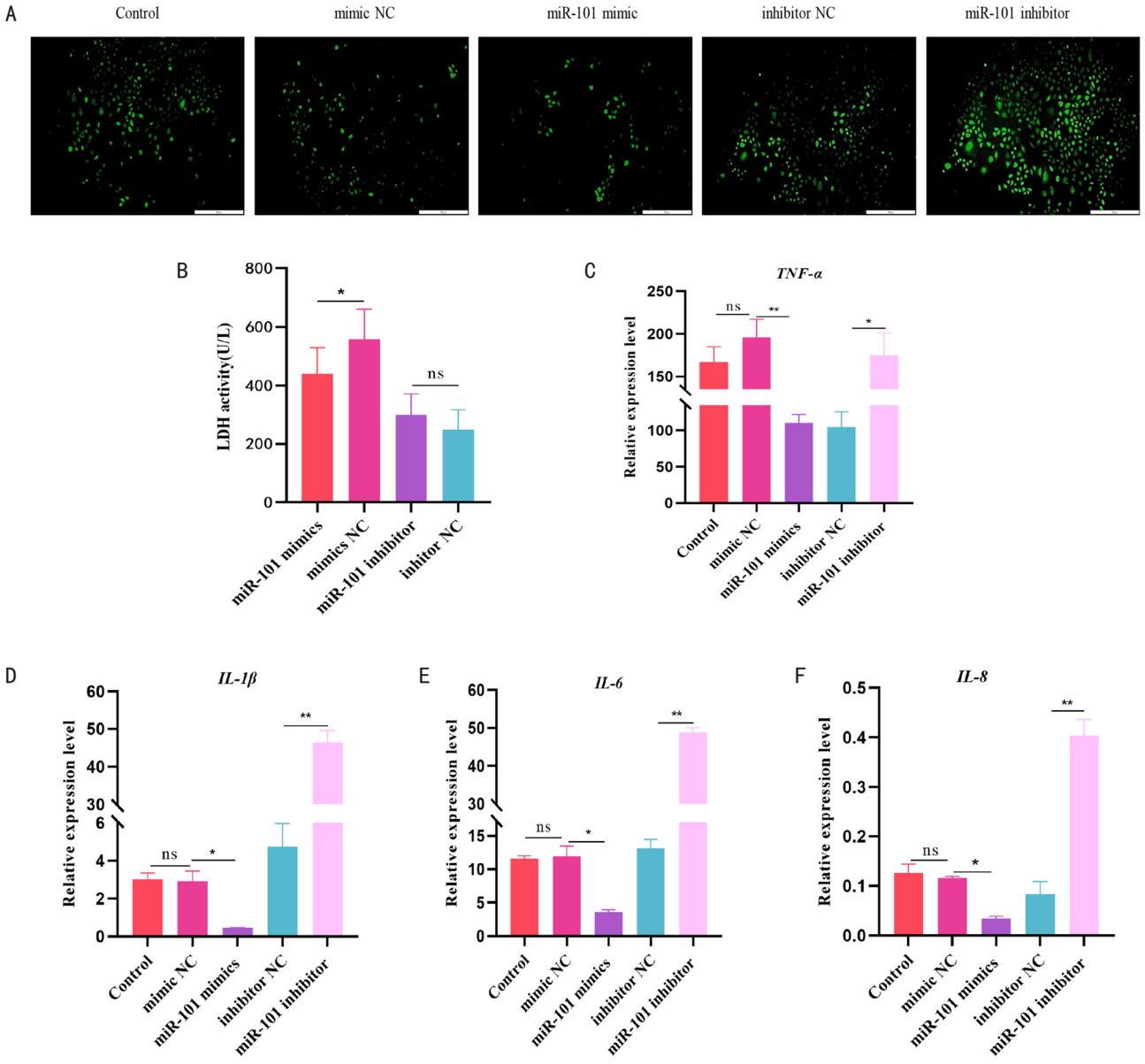

Fig. 3. Ssc-miR-101-3p overexpression attenuated the inflammatory damage in the ATII cells. (**A**) ROS levels were measured to assess apoptosis in the ATII cells transfected with miR-101-3p mimics, miR-101-3p inhibitors, or NC. (**B**) LDH activity was detected by measuring the absorbance at 450 nm. (**C–F**) qRT-PCR was used to evaluate the levels of inflammatory factors *TNF-α*, *IL-1β*, *IL-6*, and *IL-8*.

Ssc-miR-101-3p targets the 3′ UTR of *FOXO3* in ATII cells

To elucidate the regulatory mechanisms of ssc-miR-101-3p in ATII cells, three different miRNA online prediction tools—RNAhybrid(v2.1.2) + svm_light, Miranda, and TargetScan—were utilized to identify the target genes of ssc-miR-101-3p. An intersection analysis of the results from these tools revealed a total of 5037 common target genes (Supplementary Table S3). KEGG and GO functional analysis indicated significant enrichment of common target genes in the FOXO and PI3K-AKT signaling pathways (Fig. 4A,B; Supplementary Tables S4, S5). Based on pathway-based gene interaction scoring and binding site assessment principles, we identified the binding of ssc-miR-101-3p's seed sequence (CA-GACAU) to the 3'-UTR region of *FOXO3*, suggesting that *FOXO3* may be a target gene of ssc-miR-101-3p. Interestingly, we discovered a perfect match between the miRNA's nucleotides 13–18 (AUAACU) and the upstream region of the *FOXO3* binding site (AGUUAU), which may indicate an additional compensatory mechanism (Fig. 4C). To accurately confirm the regulatory mechanism of ssc-miR-101-3p on *FOXO3*, we prioritized the conserved seed region for further work. We successfully constructed wild-type and mutant FOXO3 3'UTR dual-luciferase reporter vectors. As expected, the ssc-miR-101-3p mimic significantly inhibited the luciferase activity of the wild-type FOXO3 3'UTR, while the activity level of the mutant FOXO3 3'UTR remained unchanged (Fig. 4D). Additionally, overexpression of ssc-miR-101-3p significantly suppressed

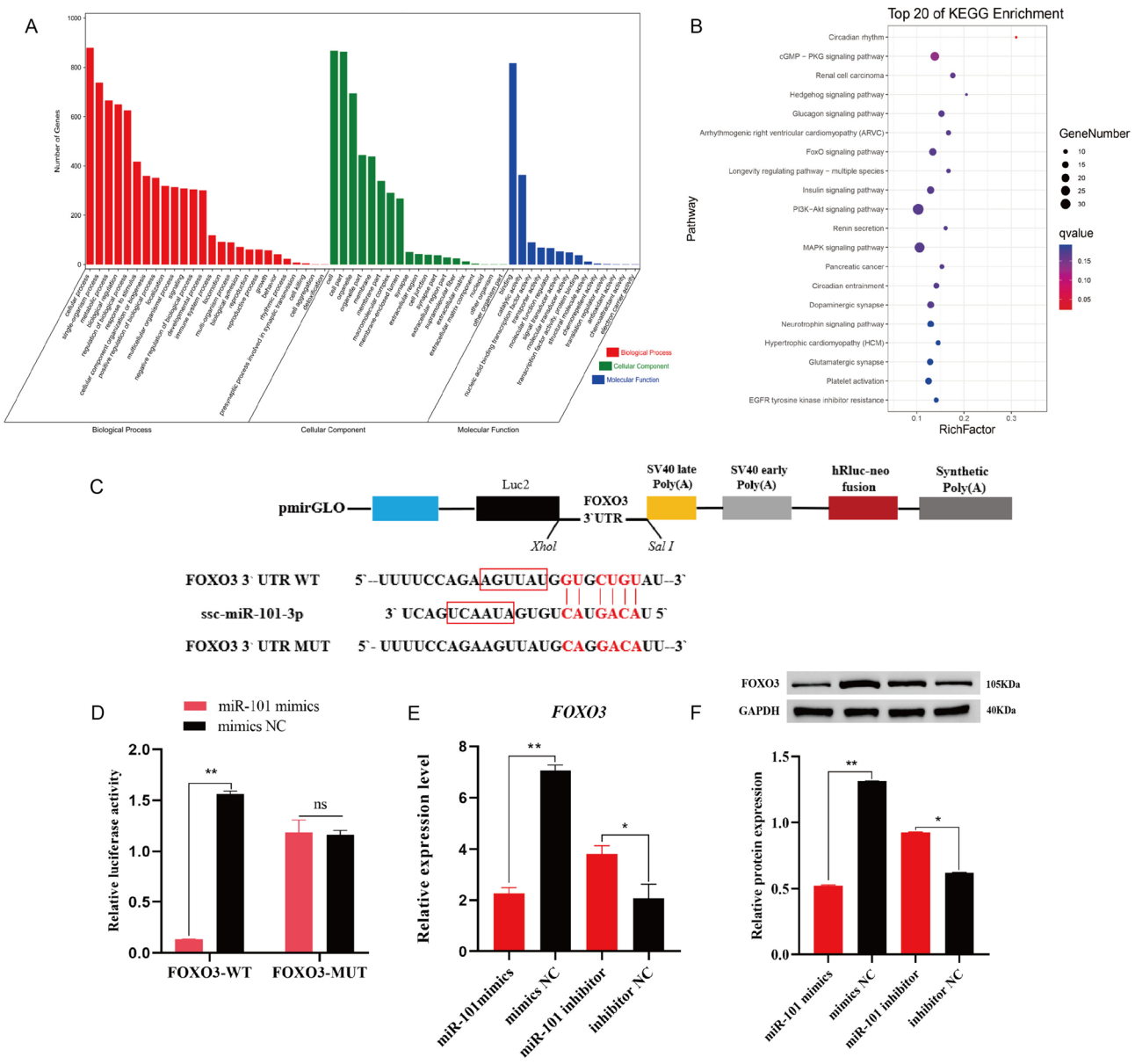

Fig. 4. Ssc-miR-101-3p directly binds to FOXO3 3`UTR *FOXO3* (**A**, **B**) GO and KEGG pathway enrichment analyses of the target genes of miR-101-3p. (**C**) The sequence in the 3′-UTR of *FOXO3* that binds to miR-101-3p, red boxes indicate additional compensation mechanisms. (**D**) Dual luciferase assay assessing the relationship between miR-101-3p and *FOXO3*. (**E**) mRNA level of *FOXO3* after transfection with miR-101-3p. (**F**) Protein levels of FOXO3 after transfection with miR-101-3p.

the mRNA and protein levels of FOXO3 in ATII cells, whereas the inhibitor of ssc-miR-101-3p significantly increased the mRNA and protein levels of FOXO3 (Fig. 4E,F). These results indicate that *FOXO3* is a direct target gene of ssc-miR-101-3p.

Effect of *FOXO3* on the proliferation and apoptosis of ATII cells in Tibetan pigs under hypoxia

To investigate the regulatory effects of *FOXO3* on ATII cell proliferation, these cells were transfected with *FOXO3* overexpression and suppression vectors, yielding significant increases or decreases in FOXO3 protein and mRNA levels, respectively (Fig. 5A,B). CCK-8 and EdU staining results illustrated that overexpression of *FOXO3* reduced cell viability and the number of EdU-positive cells. Conversely, treatment with *FOXO3* inhibitors demonstrated opposite outcomes (Fig. 4C,F–G). Flow cytometry results indicated that overexpressing *FOXO3* increased the proportion of ATII cells in the G1 phase and decreased the proportions in the S and G2 phases compared to cells transfected with pcDNA3.1 ($P < 0.05$). Furthermore, inhibition of *FOXO3* led to an increase in the percentages of S and G2 phase cells relative to cells transfected with inhibitor NC, while maintaining a higher proportion of cells in the G1 phase ($P < 0.05$) (Fig. 5D,E). Additionally, overexpression of *FOXO3* significantly upregulated *Bax* and downregulated *Bcl-2*, whereas inhibition of *FOXO3* showed reverse effects (Fig. 5H,I). Therefore, overexpression of *FOXO3* may promote hypoxia-induced apoptosis in ATII cells.

FOXO3 increases hypoxia-induced toxicity and inflammatory damage in the ATII cells

To further explore the effect of *FOXO3* in hypoxia-induced inflammation in ATII cells, we analyzed the effect of *FOXO3* knockdown and overexpression on hypoxia-induced ATII cytotoxicity by assessing the ROS levels and LDH activity. LDH activity and ROS levels were significantly increased after *FOXO3* overexpression and decreased after *FOXO3* knockdown (Fig. 6A,B). In addition, qRT-PCR results indicated that the inflammatory factors *TNF-α*, *IL-6*, *IL-8*, and *IL-1β* were differentially upregulated after transfection with pc-FOXO3 (*FOXO3* overexpression) and downregulated in varying degrees after transfection with si-FOXO3 (*FOXO3* knockdown) (Fig. 6C,D). These results suggested that *FOXO3* overexpression aggravates hypoxia-induced inflammatory damage in ATII cells.

ssc-miR-101-3p targets *FOXO3* to regulate ATII cell damage induced by hypoxia

Based on the above results, we determined that a relationship and negative functional correlation exists between ssc-miR-101-3p and *FOXO3*. We further determined whether ssc-miR-101-3p alters the effect of *FOXO3* on ATII cell proliferation and damage. ATII cells were co-transfected with ssc-miR-101-3p mimic and pc-FOXO3 vectors and with mimic NC and pc-FOXO3 as controls. CCK-8, EdU staining, and flow cytometry results indicated that ssc-miR-101-3p overexpression attenuated the inhibitory effects of *FOXO3* on cell viability, proliferation, and cell cycle (Fig. 7A,E–H). The ssc-miR-101-3p mimic and pc-FOXO3 co-transfection inhibited the expression of the proapoptotic factor *Bax* and promoted the expression of the anti-apoptotic factor *Bcl-2* (Fig. 7B,C). In addition, the co-transfection with ssc-miR-101-3p mimic and pc-FOXO3 significantly reduced the LDH activity and levels of ROS and inflammatory factors (*TNF-α*, *IL-1β*, *IL-6*, and *IL-8*) compared with the control transfection (Fig. 7D,I–J). Therefore, the above results suggested that ssc-miR-101-3p exhibits a protective effect on ATII cells by inhibiting the expression of *FOXO3*.

Discussion

High-altitude, low-oxygen environments affect mammalian physiology and pose a great challenge for mammalian survival[31]. One of the most important functions of the lung is to maintain adequate oxygenation in the body. When the lung is exposed to hypoxic environment, mitochondrial function in the lung cells is impaired, which in turn leads to increased oxidative damage in the lung[32]. Hoenderdos et al. reported that hypoxia induces a destructive phenotype in neutrophils with delayed apoptosis, impaired capacity of killing bacterial cells, and increased release of cytotoxic proteases, which in turn increases the likelihood of an inflammatory response in the organism[33]. ATII cells play an important role in maintaining alveolar integrity and function, and they may be critical for lung function and repair[34]. To determine whether hypoxic environment affects the morphology of ATII cells of Tibetan pigs, the changes in morphological structure of ATII cells were assessed using transmission electron microscopy after 48 h of hypoxia treatment in vitro. Compared with the normoxic group (21% O_2), the apoptotic features of ATII cells were obvious in the hypoxic group (2% O_2), with disappearance of lamellar vesicles, significant swelling of mitochondria, and reduction of cell membrane microvilli. This was consistent with the apoptotic morphology of rat ATII cells studied by Huang et al[35]. This indicated that long-term exposure of ATII cell to hypoxic environmental stimuli leads to apoptosis. Stimulus response is a cellular response in which the organism's own defenses are activated when exposed to any stimulus (such as hypoxia); this occurs by the regulation of expression of various RNAs (miRNA) in the cell[36]. Several studies have reported that miRNAs play a key role in coordinating many fundamental biological processes, including proliferation, apoptosis, differentiation, and metabolism[37,38]. Our previous study reported that ssc-miR-101-3p was differentially expressed in the lung tissues of Tibetan pigs at different altitudes. Therefore, it is important to explore whether porcine ssc-miR-101-3p is involved in the regulation of adaptation to hypoxic conditions in Tibetan pigs at different altitudes.

MiRNAs are involved in post-transcriptional regulation of genes and play an important role in developmental processes, cell differentiation, and immune defense in organisms[39]. miRNA expression has been reported to trigger innate immune responses in hypoxic environments and enhance host defense. Shi et al. reported that hypoxia inhibits cell cycle progression and cell proliferation in brain microvascular endothelial cells through the miR-212-3p/MCM2 axis[40]. miR-181a and miR-150 target the JAK1-STAT1/c Fos pathway that regulates immune inflammatory response and cardiomyocyte apoptosis in dendritic cells[41]. miR-760 mediates hypoxia-induced proliferation and apoptosis in the smooth muscle cells of human pulmonary artery by targeting *TLR4*[42]. These

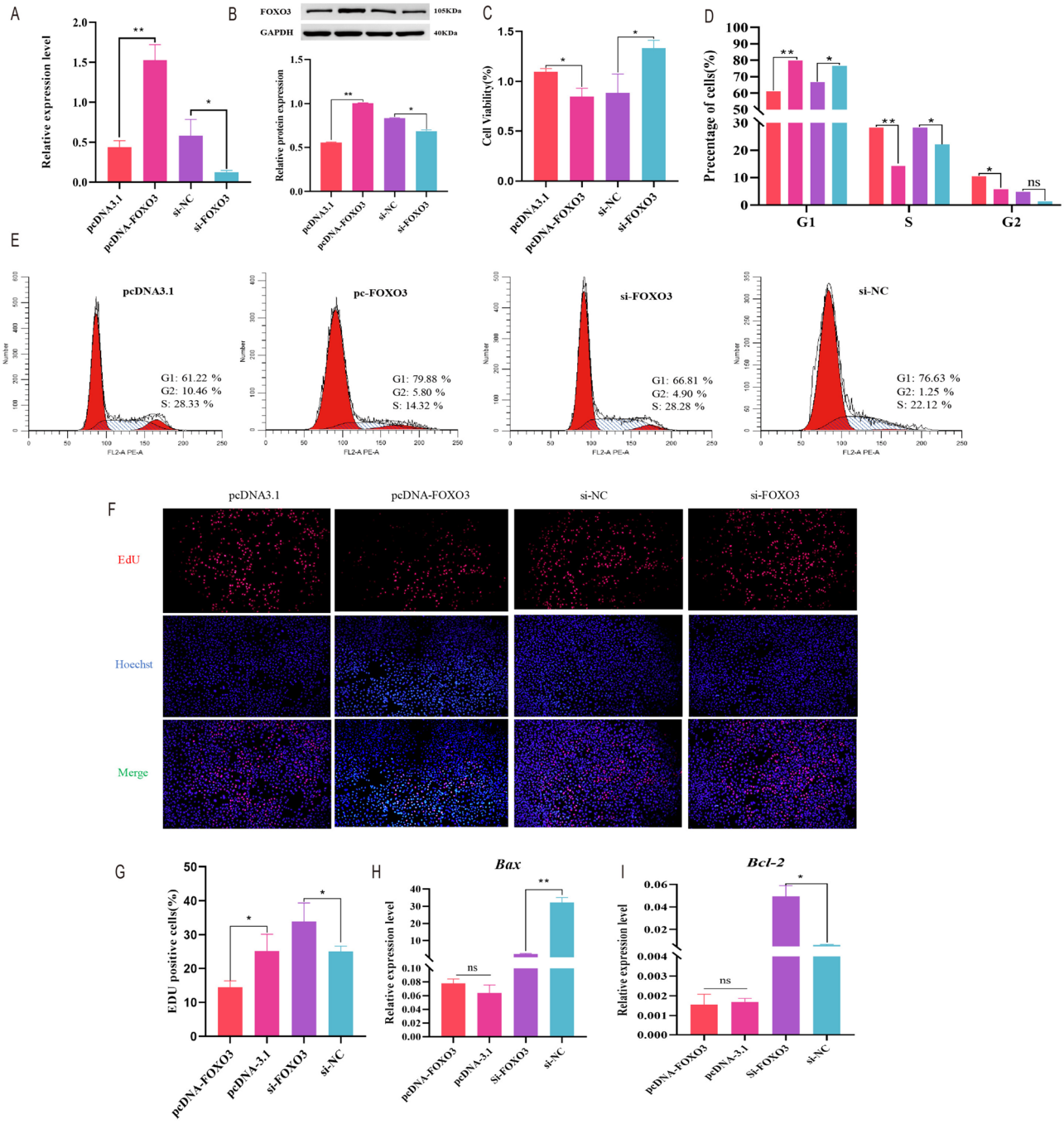

Fig. 5. *FOXO3* could regulate the survival rate and apoptosis of ATII cells. (**A**, **B**) The mRNA and protein levels of *FOXO3* were evaluated using qPCR and western blot analysis, respectively, in ATII cells after *FOXO3* overexpression or inhibition. (**C**) CCK-8 assay was used to detect the cell viability of ATII cells with *FOXO3* overexpression or inhibition. (**D**, **E**) Determination of cell cycle phase of ATII cells using flow cytometry. (**F**) EdU staining. The ATII cells in S phase were stained red with EdU, whereas the nucleus was stained blue with Hoechst. (**G**) The proportion of proliferating cells was analyzed using Image J. (**G**, **H**) qRT-PCR was used to detect the mRNA levels of apoptosis-related genes *Bax* and *Bcl-2* after *FOXO3* overexpression and interference.

findings suggested that aberrant miRNA expression is a key factor in regulating cell proliferation and apoptosis under hypoxia. Our previous study reported that ssc-miR-101-3p was significantly expressed in the lung tissue of Tibetan pigs at high altitude, suggesting that ssc-miR-101-3p may play an important role in the adaptation of Tibetan pigs to hypoxic environment. In the present study, ssc-miR-101-3p expression was significantly elevated in the ATII cells after hypoxia treatment, suggesting that ssc-miR-101-3p may be involved in the regulation of ATII cells under hypoxia. Therefore, we further verified whether ssc-miR-101-3p affected hypoxia-induced apoptosis in the ATII cells. Notably, ssc-miR-101-3p overexpression promoted ATII cell proliferation and decreased LDH activity, ROS levels, and release of proinflammatory factors, whereas ssc-miR-101-3p inhibition exhibited

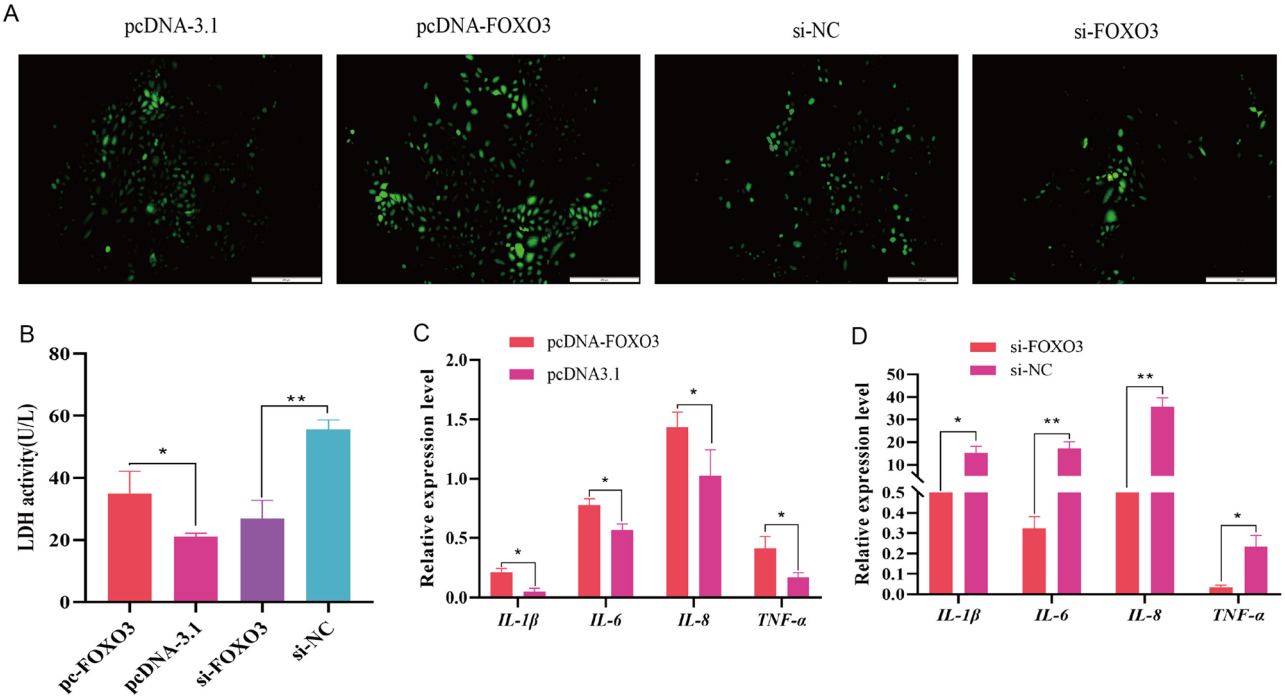

Fig. 6. *FOXO3* overexpression exacerbates inflammatory damage in ATII cells. (**A**) ROS levels were measured to assess apoptosis in ATII cells transfected with vectors for *FOXO3* overexpression or inhibition or NC. (**B**) LDH activity was assessed by measuring absorbance at 450 nm. (**C**, **D**) The transcript levels of *TNF-α*, *IL-1β*, *IL-6*, and *IL-8* were detected using qPCR after *FOXO3* overexpression or inhibition.

the opposite effect. miR-101 overexpression is reported to significantly reduce apoptosis and promote proliferation of hair follicle stem cells ($P < 0.01$) and increase mRNA and protein levels of proliferation-related (*PCNA*) and antiapoptotic (*Bcl-2*) genes[43]. miR-101 overexpression was reported to inhibit increased autophagy and apoptosis in mouse and cardiac myocytes ($P < 0.01$)[44], which is consistent with our findings. Therefore, it can be concluded that upregulation of ssc-miR-101-3p inhibits hypoxia-induced ATII cell injury.

The regulatory effects of miRNAs on cell proliferation and apoptosis are achieved by binding to target genes[45]. Xu et al. reported that prediction of target genes of miRNAs using bioinformatic softwares is a rapid and efficient method[46]. Therefore, in this study, three online software programs, namely, RNAhybrid + svm_light, TargetScan, and Miranda, were used to predict the target genes of ssc-miR-101-3p, and 5037 shared target genes were successfully predicted. GO and KEGG functional enrichment analyses indicated that the target genes were significantly enriched in FOXO and PI3K-AKT signaling pathways. The lipoylinositol 3-kinase (PI3K) and protein kinase B (AKT) signaling pathways play central roles in cell proliferation and survival. FOXO transcription factor is negatively regulated by the PI3K/AKT signaling pathway, and these pathways are directly involved in the regulation of cell proliferation and apoptosis under hypoxia[47]. In alignment with the principles of pathway-based gene interaction scoring and binding site evaluation, our study identified *FOXO3* as a candidate target gene for miR-101-3p, based on its conserved region (CA-GACAU) that binds to this microRNA. However, the binding site was discontinuous. Notwithstanding this, we uncovered a perfect pairing between the upstream region of the *FOXO3* binding site (AGUUAU) and nucleotides 13 to 18 (AUAACU) of the miRNA. This observation suggests a compensatory mechanism for less than ideal seed pairing. Research by Friedman, Jan et al. has highlighted that, beyond the seed region match, a shift of six nucleotides in either the 3' or 5' direction, offset by one nucleotide, can sometimes mediate detectable repression[48,49]. In parallel, Bartel et al. have noted that the complementarity of nucleotides 13–16 at the 3' end of the miRNA can augment the pairing within the seed region[35]. Yet, the impact of these 3'-terminal complementary pairing sites on affinity and effectiveness is negligible. Thus, we prioritized the conserved seed region for our subsequent investigations—emphasizing the significance of the core binding motif. Our conclusions were substantiated by qRT-PCR, Western blot, and dual-luciferase reporter assays, all of which collectively verified that ssc-miR-101-3p specifically targets and binds to *FOXO3*. Furthermore, *FOXO3* overexpression further exacerbated hypoxia-induced ATII cell damage; however, ssc-miR-101-3p overexpression reversed this effect. *FOXO3* is a widely studied transcription factor that plays an important role in a wide range of physiological and pathological processes by regulating a multigene regulatory network[50]. Essers et al. reported that under oxidative stress, including reduced oxygen levels, *FOXO3* is activated through signaling pathways involving Ral and JNK. This suggested that *FOXO3* activation is involved in oxidative-stress-induced apoptosis[51]. Clinical trials revealed that RG7112, an MDM2 antagonist, inhibited cancer cell growth in acute leukemia by inducing apoptosis through the reactivation of *FOXO3* under hypoxic conditions[52]. As expected, our data indicated that *FOXO3* overexpression exacerbated the hypoxia-induced inflammatory response and promoted apoptosis in ATII cells. We further explored whether ssc-miR-101-3p regulates hypoxia-induced

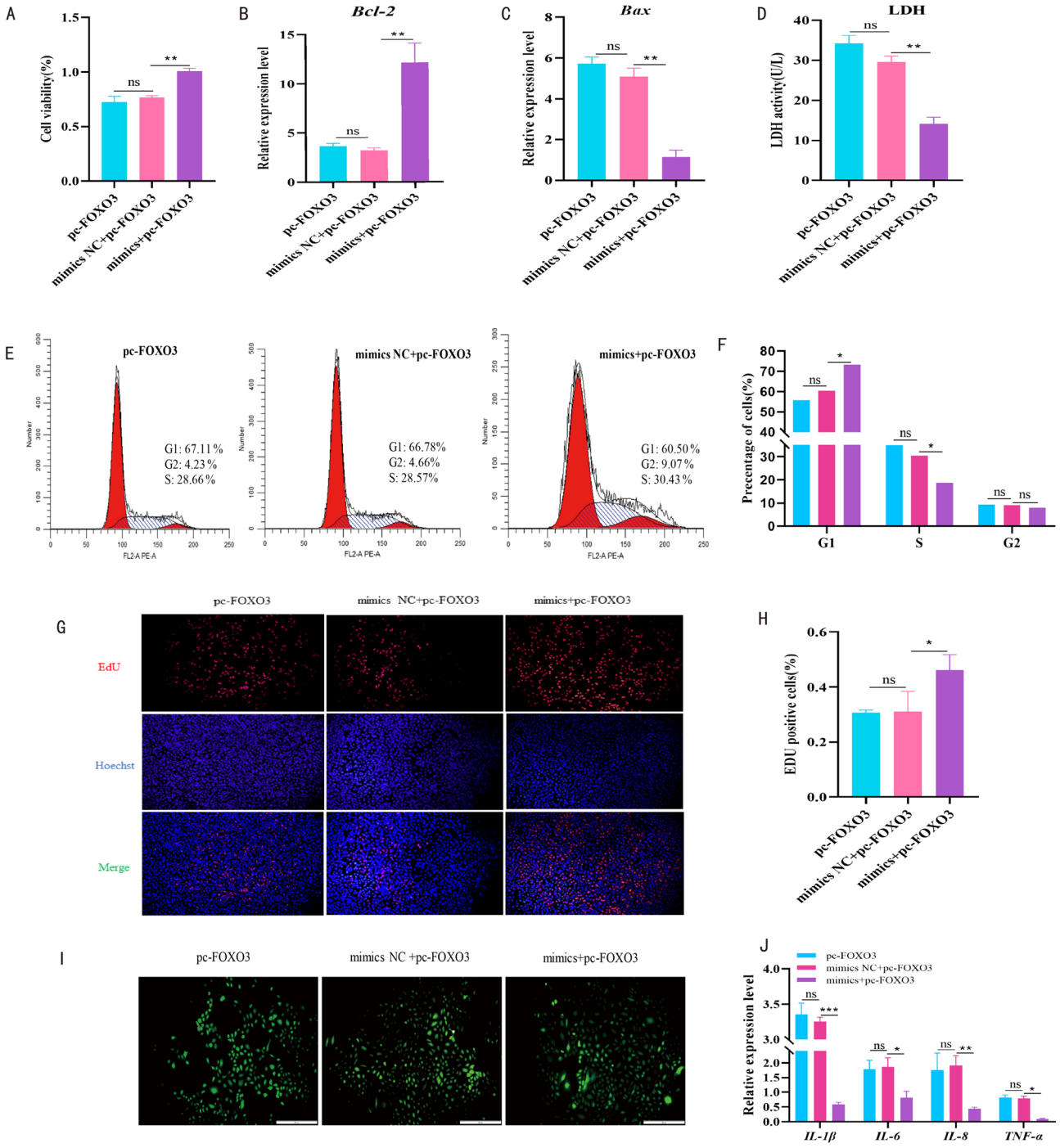

Fig. 7. Ssc-miR-101-3p regulates apoptosis and inflammatory damage in ATII cells by targeting *FOXO3*. (**A**) CCK-8 assay for ATII cell viability 48 h after miR-101-mimics and *FOXO3* overexpression plasmids were co-transfected. (**B**, **C**) Levels of apoptosis-related genes *Bax* and *Bcl-2* mRNA after combined treatment. (**D**) LDH activity was assessed by measuring absorbance 450 nm. (**E**, **F**) Determination of cell cycle phase of ATII cells co-transfected with miR-101-3p mimic and *FOXO3* overexpression plasmid using flow cytometry. (**G**) EdU staining was performed to detect the proliferation of ATII cells 48 h after co-transfection with miR-101-3p mimic and *FOXO3* overexpression plasmid. (**H**) EdU-positive cells. (**I**) ROS levels were measured to assess apoptosis in ATII cells after co-transfection. (**J**) Expression levels of *TNF-α*, *IL-1β*, *IL-6*, and *IL-8* after co-transfection.

ATII cell apoptosis by binding to *FOXO3*. The findings revealed that the roles of *FOXO3* and ssc-miR-101-3p are completely opposite in hypoxia-induced apoptosis and inflammatory response. ssc-miR-101-3p may inhibit hypoxia-induced ATII cell apoptosis and inflammatory response by targeting *FOXO3* (Fig. 8). Nevertheless,

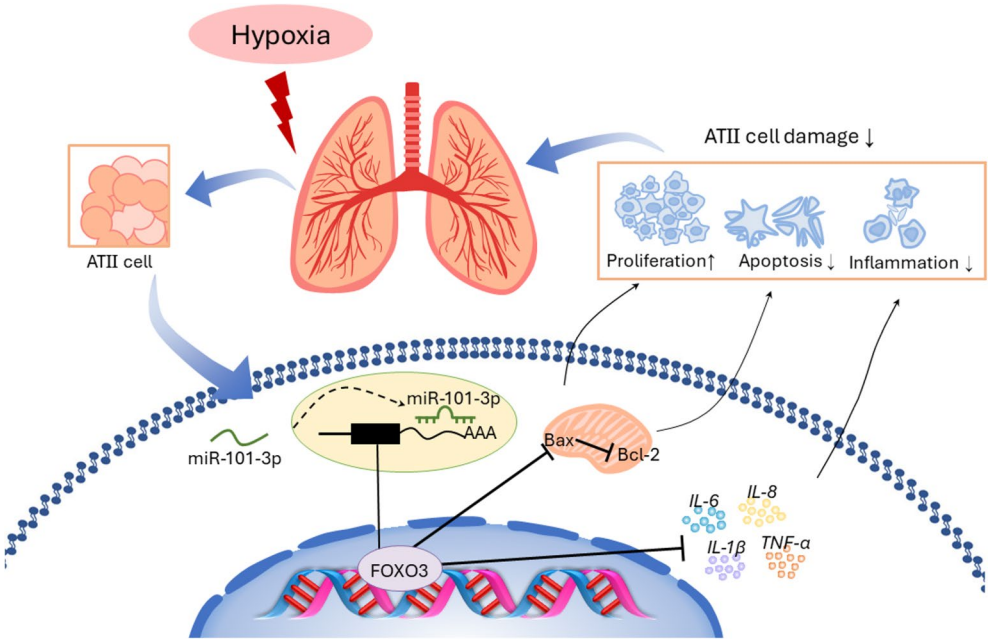

Fig. 8. Schematic representation of ssc-miR-101-3p related regulatory mechanisms affecting ATII cells in Tibetan pigs under hypoxia. Ssc-miR-101-3p targeted *FOXO3* alleviates hypoxia-induced apoptosis and inflammatory injury in ATII cells of Tibetan pigs.

we are acutely aware of the limitations inherent in our study. While the interaction between ssc-miR-101-3p and *FOXO3* in Tibetan pigs has revealed its significant role in mechanisms of hypoxic adaptation, we have yet to directly ascertain the specificity and ubiquity of this mechanism across other swine species. This realization underscores the necessity for future research to place a greater emphasis on interspecies comparative analyses, thereby enabling a comprehensive evaluation of the cross-species applicability and functional versatility of the ssc-miR-101-3p-FOXO3 interaction.

Conclusion

In conclusion, our study revealed that ssc-miR-101-3p targets 3′ UTR of *FOXO3* to alleviate hypoxia-induced inflammation and to promote cell proliferation in ATII cells of Tibetan pigs. These results provided new insights into the function of miRNAs in the ATII cells of Tibetan pigs and would help in better understanding of the regulatory mechanisms by which lung tissues of Tibetan pigs adapt to hypoxic environment.

Received: 18 November 2023; Accepted: 19 August 2024
Published online: 29 August 2024

References

1. Xu, S. *et al.* A genome-wide search for signals of high-altitude adaptation in Tibetans. *Mol. Biol. Evol.* **28**, 1003–1011 (2011).
2. Hao, G. S., Fan, Q. L., Hu, Q. Z. & Hou, Q. Research progress on the mechanism of cerebral blood flow regulation in hypoxia environment at plateau. *Bioengineered* **13**, 6353–6358 (2022).
3. Luks, A. M., Swenson, E. R. & Bartsch, P. Acute high-altitude sickness. *Eur. Respir. Rev.* **26**, 16096 (2017).
4. Chen, T., Yang, C., Li, M. & Tan, X. Alveolar hypoxia-induced pulmonary inflammation: From local initiation to secondary promotion by activated systemic inflammation. *J. Vasc. Res.* **53**, 317–329 (2016).
5. Swenson, E. R. & Bartsch, P. High-altitude pulmonary edema. *Compr. Physiol.* **2**, 2753–2773 (2012).
6. Ma, Y. F. *et al.* Population genomics analysis revealed origin and high-altitude adaptation of tibetan pigs. *Sci. Rep.* **9**, 11463 (2019).
7. Wang, M. *et al.* Detection and genetic characterization of porcine deltacoronavirus in Tibetan pigs surrounding the Qinghai-Tibet Plateau of China. *Transbound. Emerg. Dis.* **65**, 363–369 (2018).
8. Bartel, D. P. MicroRNAs: Genomics, biogenesis, mechanism, and function. *Cell* **116**, 281–297 (2004).
9. Lewis, B. P., Shih, I. H., Jones-Rhoades, M. W., Bartel, D. P. & Burge, C. B. Prediction of mammalian microRNA targets. *Cell* **115**, 787–798 (2003).
10. Soufi-Zomorrod, M. *et al.* MicroRNAs modulating angiogenesis: miR-129-1 and miR-133 act as angio-miR in HUVECs. *Tumour. Biol.* **37**, 9527–9534 (2016).
11. Ruan, W., Xu, J. M., Li, S. B., Yuan, L. Q. & Dai, R. P. Effects of down-regulation of microRNA-23a on TNF-alpha-induced endothelial cell apoptosis through caspase-dependent pathways. *Cardiovasc. Res.* **93**, 623–632 (2012).
12. Chapat, C. *et al.* Cap-binding protein 4EHP effects translation silencing by microRNAs. *Proc. Natl. Acad. Sci. USA* **114**, 5425–5430 (2017).
13. Zhang, J. P., Zhang, W. J., Yang, M. & Fang, H. Propofol attenuates lung ischemia/reperfusion injury though the involvement of the MALAT1/microRNA-144/GSK3beta axis. *Mol. Med.* **27**, 77 (2021).
14. Dai, S.-H. microRNA-145 Inhibition Upregulates SIRT1 and Attenuates Autophagy in a Mouse Model of Lung Ischemia/Reperfusion Injury via NF-κB-dependent Beclin 1. *Transplantation* **105**(3), 529–539. https://doi.org/10.1097/TP.0000000000003435 (2021).

15. Ye, C. *et al.* microRNA-223 promotes autophagy to aggravate lung ischemia-reperfusion injury by inhibiting the expression of transcription factor HIF2alpha. *Am. J. Physiol. Lung Cell Mol. Physiol.* **319**, L1–L10 (2020).
16. Yang, Y. *et al.* Transcriptome and metabolome integration provides new insights into the regulatory networks of Tibetan pig alveolar type II epithelial cells in response to hypoxia. *Front. Genet.* **13**, 812411 (2022).
17. Deng, A. *et al. FoxO3* transcription factor promotes autophagy after oxidative stress injury in HT22 cells. *Can. J. Physiol. Pharmacol.* **99**, 627–634 (2021).
18. Morris, B. J. W. D. *FOXO3*: A major gene for human longevity - a mini-review. *Gerontology* **61**(6), 515–525 (2015).
19. Du, W. W. *et al.* Induction of tumor apoptosis through a circular RNA enhancing Foxo3 activity. *Cell Death Differ.* **24**, 357–370 (2017).
20. Yin, Z. *et al.* MiRNA-96-5p impacts the progression of breast cancer through targeting FOXO3. *Thorac. Cancer* **11**, 956–963 (2020).
21. Cao, M. Q. *et al.* miR-182-5p promotes hepatocellular carcinoma progression by repressing FOXO3a. *J. Hematol. Oncol.* **11**, 12 (2018).
22. Meng, L., Xing, Z., Guo, Z., Qiu, Y. & Liu, Z. Hypoxia-induced microRNA-155 overexpression in extracellular vesicles promotes renal cell carcinoma progression by targeting *FOXO3*. *Aging (Albany NY)* **13**, 9613–9626 (2021).
23. Khan, P. *et al.* Culture of human alveolar epithelial type II cells by sprouting. *Respir. Res.* **19**, 204 (2018).
24. Dehmel, S. *et al.* microRNA expression profile of purified alveolar epithelial type II cells. *Genes (Basel)* **13**, 1420 (2022).
25. Yang, Y. *et al.* Post-transcriptional regulation through alternative splicing in the lungs of Tibetan pigs under hypoxia. *Gene* **819**, 146268 (2022).
26. Shi, S. *et al.* Totipotency of miR-184 in porcine granulosa cells. *Mol. Cell Endocrinol.* **558**, 111765 (2022).
27. Rao, X., Huang, X., Zhou, Z. & Lin, X. An improvement of the 2^(-delta delta CT) method for quantitative real-time polymerase chain reaction data analysis. *Biostat. Bioinforma. Biomath.* **3**, 71–85 (2013).
28. Kanehisa, M., Furumichi, M., Sato, Y., Kawashima, M. & Ishiguro-Watanabe, M. KEGG for taxonomy-based analysis of pathways and genomes. *Nucleic Acids Res.* **51**, D587–D592 (2023).
29. Kanehisa, M. Toward understanding the origin and evolution of cellular organisms. *Protein Sci.* **28**, 1947–1951 (2019).
30. Yang, Y. *et al.* Characterization of circRNA-miRNA-mRNA networks regulating oxygen utilization in type II alveolar epithelial cells of Tibetan pigs. *Front. Mol. Biosci.* **9**, 854250 (2022).
31. Zhu, K., Ge, D., Wen, Z., Xia, L. & Yang, Q. Evolutionary genetics of hypoxia and cold tolerance in mammals. *J. Mol. Evol.* **86**, 618–634 (2018).
32. Araneda, O. F. & Tuesta, M. Lung oxidative damage by hypoxia. *Oxid. Med. Cell Longev.* **2012**, 856918 (2012).
33. Hoenderdos, K. S115 The effects of hypoxia on neutrophil-mediated tissue damage in the lung. *Thorax* **68**(Suppl 3), A60. https://doi.org/10.1136/thoraxjnl-2013-204457.122 (2013).
34. Yazicioglu, T. *et al.* Aging impairs alveolar epithelial type II cell function in acute lung injury. *Am. J. Physiol. Lung Cell Mol. Physiol.* **319**, L755–L769 (2020).
35. Huang, R. *et al.* Inhibition of the cGAS-STING pathway attenuates lung ischemia/reperfusion injury via regulating endoplasmic reticulum stress in alveolar epithelial type II cells of rats. *J. Inflamm. Res.* **15**, 5103–5119 (2022).
36. Chan, S. Y. & Loscalzo, J. MicroRNA-210: A unique and pleiotropic hypoxamir. *Cell Cycle* **9**, 1072–1083 (2010).
37. Bartel, D. P. MicroRNAs: Target recognition and regulatory functions. *Cell* **136**, 215–233 (2009).
38. Mendell, J. T. & Olson, E. N. MicroRNAs in stress signaling and human disease. *Cell* **148**, 1172–1187 (2012).
39. Chang, M. *et al.* Differential expression of miRNAs in the body wall of the sea cucumber *Apostichopus japonicus* under heat stress. *Front. Physiol.* **13**, 929094 (2022).
40. Shi, Q. *et al.* Hypoxia inhibits cell cycle progression and cell proliferation in brain microvascular endothelial cells via the miR-212-3p/MCM2 Axis. *Int. J. Mol. Sci.* **24**(3), 2788. https://doi.org/10.3390/ijms24032788 (2023).
41. Zhu, J. *et al.* miR-181a and miR-150 regulate dendritic cell immune inflammatory responses and cardiomyocyte apoptosis via targeting JAK1-STAT1/c-Fos pathway. *J. Cell Mol. Med.* **21**, 2884–2895 (2017).
42. Yang, Y. Z. *et al.* miR-760 mediates hypoxia-induced proliferation and apoptosis of human pulmonary artery smooth muscle cells via targeting TLR4. *Int. J. Mol. Med.* **42**, 2437–2446 (2018).
43. Jingwen, Q. *et al.* Effect of miR-101 on the proliferation and apoptosis of goat hair follicle stem cells. *Genes* **13**(6), 1035. https://doi.org/10.3390/genes13061035 (2022).
44. Li, Q., Gao, Y., Zhu, J. & Jia, Q. MiR-101 attenuates myocardial infarction-induced injury by targeting DDIT4 to regulate autophagy. *Curr. Neurovasc. Res.* **17**, 123–130 (2020).
45. Gao, Z., Zhou, H., Wang, Y., Chen, J. & Ou, Y. Regulatory effects of lncRNA ATB targeting miR-200c on proliferation and apoptosis of colorectal cancer cells. *J. Cell Biochem.* **121**, 332–343 (2020).
46. Linna, X., Yuan, H., Wang, Z., Zhao, S. & Yang, Y. Ssc-miR-141 attenuates hypoxia-induced alveolar type II epithelial cell injury in Tibetan pigs by targeting PDCD4. *Genes* **13**(12), 2398. https://doi.org/10.3390/genes13122398 (2022).
47. Zhang, M. & Zhang, X. The role of PI3K/AKT/FOXO signaling in psoriasis. *Arch. Dermatol. Res.* **311**, 83–91 (2019).
48. Friedman, R. C., Farh, K. K., Burge, C. B. & Bartel, D. P. Most mammalian mRNAs are conserved targets of microRNAs. *Genome Res.* **19**, 92–105 (2009).
49. Jan, C. H., Friedman, R. C., Ruby, J. G. & Bartel, D. P. Formation, regulation and evolution of Caenorhabditis elegans 3'UTRs. *Nature* **469**, 97–101 (2011).
50. Bernardo, V. S., Torres, F. F. & Da, S. D. *FoxO3* and oxidative stress: A multifaceted role in cellular adaptation. *J. Mol. Med. (Berl).* **101**, 83–99 (2023).
51. Essers, M. A. *et al.* FOXO transcription factor activation by oxidative stress mediated by the small GTPase Ral and JNK. *Embo. J.* **23**, 4802–4812 (2004).
52. Andreeff, M. K. K. R. Results of the phase 1 trial of rg7112, a small-molecule mdm2 antagonist, in acute leukemia. *Blood* **6**, 1035 (2022).

Acknowledgements

We are very grateful to Shengguo Zhao for carefully checking and reading the manuscript, to Genedenovo Biotechnology Limited (Guangzhou, China) for providing us with sequencing data. In addition, the authors would like to thank all reviewers who participated in the review of the manuscript.

Author contributions

Y.N. and S.G. were the leader of the whole project, providing financial support and experimental conceptualization. H.N. was involved in data analysis, statistical analysis, language revision, journal selection, manuscript submission and revision. X.B. and B.P. were involved in the design and implementation of the experiments. Y.N. provided guidance and assistance in animal management, sample collection and analysis. J.Q. and C.X. were responsible for the implementation of the experiments, guiding students in sample collection and analysis, and writing the paper. All authors contributed to the article and approved the submitted version.

Funding
The study was supported by the Gansu Agricultural University, College of Animal Science and Technology, doctoral research start-up fund project, GAU-DK-QNJJ-202301.

Competing interests
The authors declare no competing interests.

Additional information
Supplementary Information The online version contains supplementary material available at https://doi.org/10.1038/s41598-024-70510-7.

Correspondence and requests for materials should be addressed to Y.Y.